

# LoS spatial multiplexing and beamforming using uniform circular array of subarrays

Yuri Jeon\*, Minhyun Kim\*, Gye-Tae Gil<sup>†</sup> and Yong H. Lee\*

\*Dept. of Electrical Engineering, Korea Advanced Institute of Science and Technology (KAIST), Daejeon, Korea

<sup>†</sup>KAIST Institute for Information Technology Convergence (KI ITC), Daejeon, Korea

Email: {yuri0703, mhkim}@stein.kaist.ac.kr, {gategil,yohlee}@kaist.ac.kr

**Abstract**—We propose the use of uniform circular array of subarrays (UCA-SAs) for millimeter wave (MMW) communication systems over line of sight (LoS) channels and design beamforming coefficients for each subarray. Specifically, for a UCA-SA consisting of  $N_s$  subarrays, which are  $M \times M$  square arrays, the beamforming coefficients are designed so that the  $N_s \times N_s$  effective channel becomes circulant. To this end, we first show that the UCA-SA can be decomposed into  $M^2$  concentric UCAs having  $N_s$  antenna elements. Then, based on this result, we show that the set of beamforming coefficients making the effective channel circulant consist of identical values. The proposed UCA-SA system employs this type of beamformers, called the constant beamformers. The effective channel of the proposed UCA-SA system can be diagonalized by the discrete Fourier transform (DFT) precoder and the inverse DFT (IDFT) combiner, without the knowledge of channel state information (CSI) at the transmitter. This indicates that constant beamformers are optimal beamformers maximizing the  $N_s \times N_s$  effective channel's mutual information. Simulation results show that the proposed UCA-SA can outperform the conventional UCA with  $N_s M^2$  antenna elements which are equally spaced on a ring.

## I. INTRODUCTION

Recently, UCAs have been recognized as a useful alternative to popular arrays such as ULAs in wireless communication systems over LoS channels. A salient feature of an  $N \times N$  UCA-based MIMO system in LoS channels is that its channel matrix can be modeled as a circulant matrix [1], [2], and thus the channel can be diagonalized by employing the N-point DFT precoder and IDFT combiner at the transmitter and receiver, respectively. Since the precoder can be fixed at the DFT matrix irrespective of the array size and the communication range, this system does not require CSI feedback for precoder design [2]. It has been observed in [3] that the UCA-based MIMO system with DFT precoder and IDFT combiner well approximates the orbital angular momentum (OAM) system in radio beams.

In contrast to the conventional view that LoS MIMO channels are rank-deficient, the results in [4]-[7] indicate that full-rank channel matrices with identical singular values can be achieved by optimizing antenna placement. For a ULA-based LoS MIMO system with Tx and Rx arrays which are spaced far enough apart, the antenna spacing required for achieving

the full-rank characteristic increases with the communication range and decreases with the carrier frequency. In the case of UCA-based LoS MIMO, similar statement holds if the number of antennas  $N$  is either three or four ( $N \in \{3, 4\}$ ) [2]: in this case, the antenna diameters need to be adjusted depending on the communication range and carrier frequency. For larger values of  $N$ , it has been shown through an asymptotic analysis with  $N \rightarrow \infty$  that the UCA-based MIMO channel cannot achieve the full-rank and contains jagged singular values, where some of them can be too small to be used for spatial multiplexing [1]. However, this result indicates that a larger spatial multiplexing gain, greater than four, can be achieved for UCAs by increasing the UCA diameter and by employing more antennas than four ( $N > 4$ ).

Array of subarray architectures have been proposed for MIMO systems over millimeter wave (MMW) channels where LoS components are dominant [8]. In this architecture,  $N_s$  uniformly spaced subarrays are employed to provide the spatial multiplexing gain of  $N_s$ , while each subarray provides beamforming gain. The transmitter of this system sends a single data stream from each subarray; the subarrays perform beamforming along the  $N_s$  LoS paths to the receiver which are assumed to be known. The size of the array of subarrays is governed by the subarray spacing, because antenna elements in each subarray can be packed into a very small area, due to the short wave-length of MMW channels. In this LoS MIMO system, the dimension of the effective channel is  $N_s \times N_s$ , and the full-rank  $N_s$  can be achieved by adjusting the subarray spacing. One obvious drawback of this ULA-based system is that the effective channel cannot be diagonalized unless the CSI is known at the transmitter.

In this paper, we propose the use of array of subarrays for UCA-based MIMO systems over MMW LoS channels. The proposed UCA with subarrays is called the uniform circular array of subarrays (UCA-SA). We employ  $N_s$  subarrays where each subarray is an  $M \times M$  square array and determine the beamforming coefficients of the subarrays so that the  $N_s \times N_s$  effective channel matrix becomes a circulant matrix. To this end, we first show that the UCA-SA system can be decomposed into  $M^2$  concentric UCA systems; based on this result, we then show that a set of beamforming coefficients making the effective channel circulant consists of identical values (for example, all 1s). We call this type of beamformers the *constant*

This work was supported by ICT R&D program of MSIP/IITP. [B0101-15-1372 , Development of Mobile Multi-mode Transmission Technology based on Spatial Spreading]

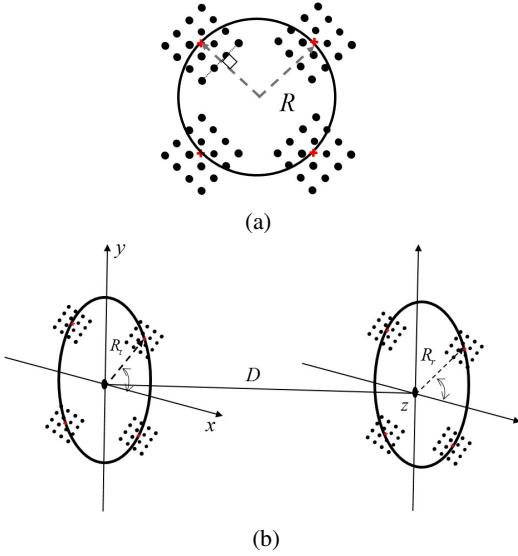


Fig. 1: (a) UCA-SA with  $N_s = M = 4$ . Here  $R$  is either  $R_t$  or  $R_r$ . (b) UCA-SA coordinate system with  $N_s = 4$ .

beamformer. The effective channel of the proposed UCA-SA with constant beamformers can be diagonalized without the knowledge of CSI at the transmitter, as in the conventional UCA-based LoS MIMO systems, indicating that the constant beamformers are optimal beamformers maximizing the  $N_s \times N_s$  effective channel's mutual information. Through computer simulation, we compare the mutual information of the proposed UCA-SA with that of the conventional  $N_s M^2 \times N_s M^2$  UCA with eigenmode communication where both the systems assume equal power control and employ UCAs with identical diameters. The results show that the proposed UCA-SA can outperform the benchmark eigenmode UCA system when  $N_s = 4$  and the diameters of UCA-SA satisfy the full-rank condition in [2].

The organization of this paper is as follows. Section II presents the system model, and Section III shows that the UCA-SA system having  $M^2$  antennas per subarray can be decomposed into  $M^2$  concentric sub-UCA systems. In section IV, it is shown that the constant beamformers can diagonalize the effective channel of the UCA-SA system. Simulation results are presented in Section V. Finally, the conclusion is described in Section VI.

*Notations:* Bold upper-case  $\mathbf{A}$  denotes a matrix and bold lower-case  $\mathbf{a}$  denotes a vector.  $\text{diag}(\mathbf{A}_1, \dots, \mathbf{A}_N)$  denotes a block diagonal matrix whose diagonal entries are given by  $\{\mathbf{A}_1, \dots, \mathbf{A}_N\}$ .  $\text{Tr}(\mathbf{A})$  is the trace and  $\text{vec}(\mathbf{A})$  represents a column vector achieved by the vectorization of a matrix  $\mathbf{A}$ .  $\mathbf{A}_{mn}$  is the sub-matrix of a matrix  $\mathbf{A}$ .  $\mathbf{I}_N$  denotes the  $N \times N$  identity matrix.

## II. SYSTEM MODEL

We consider a UCA-SA system consisting of  $N_s$  subarrays, where each subarray is an  $M \times M$  square  $\lambda/2$ -spacing array and  $\lambda$  is the carrier wavelength. The total number of antennas

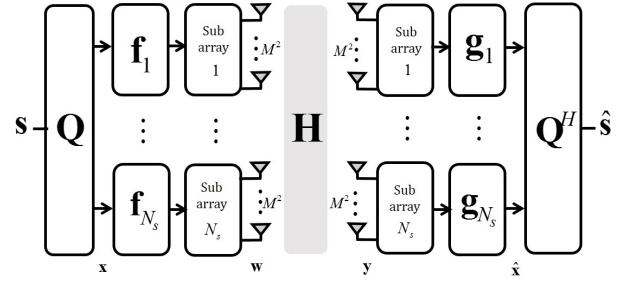


Fig. 2: UCA-SA system. The transmitter employs the beamformer  $\mathbf{F}$  and the DFT precoder  $\mathbf{Q}$ ; the receiver employs the beamformer  $\mathbf{G}^H$  and the IDFT decoder  $\mathbf{Q}^H$

per UCA is given by  $N = N_s M^2$ . The radii of transmit and receive UCA-SAs are denoted as  $R_t$  and  $R_r$ , respectively, and the center of each transmit (receive) subarray is uniformly located on a ring of radius  $R_t$  ( $R_r$ ) (Fig. 1(a)). The angle of rotation of each subarray is determined so that one side of the subarray is perpendicular to the line connecting the center of the subarray and that of UCA-SA. It is assumed that the size of subarray is much smaller than that of UCA-SA: specifically,  $(M-1)\lambda \ll R_t$  and  $R_r$ . The antenna coordinate system of the UCA-SA system is illustrated in Fig. 1(b). In this figure, the  $z$ -axis is taken in the direction from the center of the transmit UCA to the center of the receive UCA; the transmit UCA is placed in the  $xy$ -plane; and the receive UCA is placed parallel to the  $xy$ -plane.

The UCA-SA system is illustrated in Fig. 2. To diagonalize the channel  $\mathbf{H} \in \mathbb{C}^{N_s M^2 \times N_s M^2}$ , we employ transmit and receive beamformers  $\mathbf{F} \in \mathbb{C}^{N_s M^2 \times N_s}$  and  $\mathbf{G}^H \in \mathbb{C}^{N_s \times N_s M^2}$ , respectively, and design  $\mathbf{F}$  and  $\mathbf{G}^H$  so that the effective channel  $\mathbf{G}^H \mathbf{H} \mathbf{F}$  becomes a circulant matrix and can be diagonalized via DFT/IDFT (Fig. 2). The received signal in complex baseband can be modeled as

$$\mathbf{y} = \mathbf{H} \mathbf{F} \mathbf{x} + \mathbf{n} = \mathbf{H} \mathbf{w} + \mathbf{n} \quad (1)$$

where  $\mathbf{x} = \mathbf{Q} \mathbf{s}$ ;  $\mathbf{Q} \in \mathbb{C}^{N_s \times N_s}$  is the DFT precoding matrix;  $\mathbf{s} \in \mathbb{C}^{N_s \times 1}$  is the information vector;  $\mathbf{w} = \mathbf{F} \mathbf{x}$ ; and  $\mathbf{n} \in \mathbb{C}^{N_s M^2 \times 1}$  is a vector of complex additive white Gaussian noise (AWGN) with zero mean and unit variance. The received signal is passed through the receive beamformer  $\mathbf{G}^H$  and the IDFT combiner,  $\mathbf{Q}^H$ , to yield  $\hat{\mathbf{s}} = \mathbf{Q}^H \hat{\mathbf{x}}$  where

$$\hat{\mathbf{x}} = \mathbf{G}^H \mathbf{y} = \mathbf{G}^H \mathbf{H} \mathbf{F} \mathbf{x} + \mathbf{G}^H \mathbf{n}. \quad (2)$$

The transmit and receive beamforming matrices are given by

$$\mathbf{F} = \text{diag}(\mathbf{f}_1, \dots, \mathbf{f}_{N_s}) \quad (3)$$

and

$$\mathbf{G} = \text{diag}(\mathbf{g}_1, \dots, \mathbf{g}_{N_s}) \quad (4)$$

where  $\mathbf{f}_m = \text{vec}(\mathbf{F}_m) \in \mathbb{C}^{M^2 \times 1}$ ;  $\mathbf{g}_n = \text{vec}(\mathbf{G}_n) \in \mathbb{C}^{M^2 \times 1}$ ;  $\mathbf{F}_m \in \mathbb{C}^{M \times M}$  and  $\mathbf{G}_n \in \mathbb{C}^{M \times M}$  are the beamforming matrices of the  $m^{\text{th}}$  transmit and  $n^{\text{th}}$  receive subarrays, respectively.

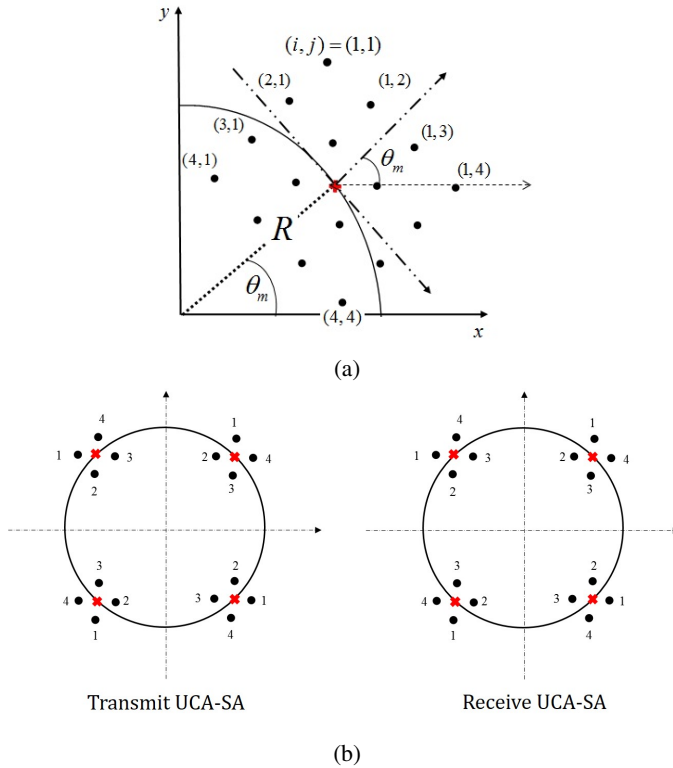


Fig. 3: (a) Coordinates of antenna elements when  $M = 4$ . (b) Decomposition of a UCA-SA system with  $N_s = 4, M = 2$  into four UCA sub-systems. Here antennas with identical indices form a UCA sub-system.

### III. SUB-UCA BASED REPRESENTATION

The UCA-SA with  $N_s$  subarrays consisting of  $M^2$  antennas per subarray can be represented as  $M^2$  concentric sub-UCAs having  $N_s$  antennas per sub-UCA, as shown below.

**Lemma 1.** *The antennas of transmit/receive UCA-SA are located on  $M^2/2$  and  $M(M+1)/2$  concentric rings when  $M$  is even and odd, respectively; and the transmit/receive UCA-SA can be decomposed into  $M^2$  concentric sub-UCAs with  $N_s$  antennas per sub-UCA.*

*Proof.* Let  $d_c(i, j)$  denote the distance between the  $(i, j)^{th}$  antenna of a subarray and the center of UCA-SA. Referring to the antenna indices shown in Fig. 3(a), we can see that  $d_c(i, j) = d_c(i, M - j + 1)$  where  $i \in \{1, 2, \dots, M\}, j \in \{1, 2, \dots, M/2\}$  for even  $M$  and  $j \in \{1, 2, \dots, (M-1)/2, (M+1)/2\}$  for odd  $M$ . When  $M$  is even, the number of concentric rings is  $M^2/2$  and there are  $2N_s$  antennas located on each ring. The  $2N_s$  antennas on each ring can be viewed as a combination of two concentric sub-UCAs with  $N_s$  antennas, and the total number of concentric sub-UCAs is  $M^2$ . Similar statement holds for odd  $M$ . When  $M$  is odd,  $2N_s$  antennas are located on a ring with radius  $d_c(i, j)$  if  $j \in \{1, 2, \dots, (M-1)/2\}$ , and only  $N_s$  antenna are located if  $j = (M+1)/2$ . Thus the number of concentric rings is

$M(M-1)/2 + M = M(M+1)/2$  and the total number of concentric sub-UCAs with  $N_s$  antennas per sub-UCA is also  $M^2(M(M-1) + M = M^2)$ . Thus, as in the case of even  $M$ , the UCA-SA with odd  $M$  can be decomposed into  $M^2$  sub-UCAs.  $\square$

Since the numbers of transmit and receive sub-UCAs are equal, we can pair transmit/receive sub-UCAs and form UCA sub-systems (for example, see Fig. 3(b)) and form the channel between the transmit and receive sub-UCAs. Let  $\tilde{\mathbf{H}}_{nm}$  denote the  $N_s \times N_s$  channel matrix between the  $m^{th}$  transmit sub-UCA and the  $n^{th}$  receive sub-UCA where both  $m$  and  $n$  are in between 1 and  $M^2$ . Then  $\tilde{\mathbf{H}}_{nm}$  is a circulant matrix, because a pair of transmit and receive sub-UCAs with the same number of antennas forms a circulant channel matrix if they are concentric and vertical to the z-axis, irrespective of their sizes and angles of rotation [1]-[3]. The overall channel, denoted as  $\tilde{\mathbf{H}} \in \mathbb{C}^{N_s M^2 \times N_s M^2}$ , written in terms of  $\tilde{\mathbf{H}}_{nm}$  is given by

$$\tilde{\mathbf{H}} = \begin{bmatrix} \tilde{\mathbf{H}}_{11} & \tilde{\mathbf{H}}_{12} & \cdots & \tilde{\mathbf{H}}_{1M^2} \\ \tilde{\mathbf{H}}_{21} & \tilde{\mathbf{H}}_{22} & \cdots & \tilde{\mathbf{H}}_{2M^2} \\ \vdots & \vdots & \ddots & \vdots \\ \tilde{\mathbf{H}}_{M^2 1} & \tilde{\mathbf{H}}_{M^2 2} & \cdots & \tilde{\mathbf{H}}_{M^2 M^2} \end{bmatrix} \quad (5)$$

The relation between  $\tilde{\mathbf{H}}$  in (5) and  $\mathbf{H}$  in (1) will be examined shortly.

### IV. CHANNEL DIAGONALIZATION

In this section, we show that the constant beamformers make the effective channel  $\mathbf{G}^H \mathbf{H} \mathbf{F}$  in (2) circulant.

**Theorem 1.** *The effective channel  $\mathbf{G}^H \mathbf{H} \mathbf{F} \in \mathbb{C}^{N_s \times N_s}$  in (2) becomes a circulant matrix if*

$$\mathbf{F} = \text{diag}[\mathbf{1}_{M^2}, \dots, \mathbf{1}_{M^2}] \quad \text{and} \quad \mathbf{G}^H = \mathbf{F}^T \quad (6)$$

where  $\mathbf{1}_{M^2}$  is the  $M^2 \times 1$  vector consisting of all 1s.

The conditions in (6) indicate that all coefficients of transmit and receive beamformers are equal to 1, which result in constant beamformers. In what follows, this theorem is proved by showing the equivalence between the UCA-SA system in Fig. 2 and that in Fig. 4 illustrating the sub-UCA based representation.

Suppose that, the precoder  $\tilde{\mathbf{F}} \in \mathbb{C}^{N_s M^2 \times N_s}$  in Fig. 4 is given by

$$\tilde{\mathbf{F}} = [\mathbf{I}_{N_s}, \dots, \mathbf{I}_{N_s}]^T, \quad (7)$$

and then the output of the precoder, denoted as  $\tilde{\mathbf{w}} \in \mathbb{C}^{N_s M^2 \times 1}$ , is written as

$$\tilde{\mathbf{w}} = [\mathbf{x}, \dots, \mathbf{x}]^T. \quad (8)$$

Each  $\mathbf{x} \in \mathbb{C}^{N_s \times 1}$  in  $\tilde{\mathbf{w}}$  serves as the input to a sub-UCA, and  $N_s$  elements of  $\mathbf{x}$  are simultaneously transmitted through the  $N_s$  antennas of each sub-UCA. The received signal  $\tilde{\mathbf{y}} \in \mathbb{C}^{N_s M^2 \times 1}$  is represented as

$$\tilde{\mathbf{y}} = \tilde{\mathbf{H}} \tilde{\mathbf{w}} + \tilde{\mathbf{n}} = \tilde{\mathbf{H}} \tilde{\mathbf{F}} \mathbf{x} + \tilde{\mathbf{n}} \quad (9)$$

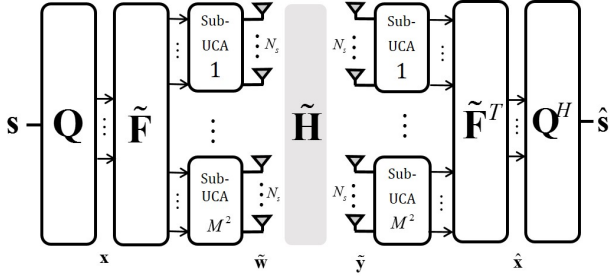


Fig. 4: UCA-SA system represented by using sub-UCAs.

where  $\tilde{\mathbf{w}} = \tilde{\mathbf{F}}\mathbf{x}$  and  $\tilde{\mathbf{n}}$  is AWGN associated with the sub-UCAs. The received signal is passed through the combiner  $\tilde{\mathbf{F}}^T$  to yield  $\tilde{\mathbf{F}}^T\tilde{\mathbf{y}}$ . Our objective is to prove that  $\tilde{\mathbf{F}}^T\tilde{\mathbf{y}}$  is identical to  $\hat{\mathbf{x}}$  in (2) for the UCA-SA systems with constant beamformers. To this end, we first examine the relation between  $\mathbf{w}$  in (1) and  $\tilde{\mathbf{w}}$  in (8). Let  $x_j$  denote the  $j^{\text{th}}$  entry of  $\mathbf{x}$ ,  $j \in \{1, \dots, N_s\}$ . When the UCA-SA employs constant beamformers,

$$\mathbf{w} = \underbrace{[x_1 \cdots x_1]}_{M^2}, \underbrace{[x_2 \cdots x_2]}_{M^2}, \dots, \underbrace{[x_{N_s} \cdots x_{N_s}]}_{M^2}^T \quad (10)$$

and the number of  $x_j$ s in  $\mathbf{w}$  and that in  $\tilde{\mathbf{w}}$  are the same and given by  $M^2$ . This holds for all  $j$ , and thus  $\mathbf{w}$  can be obtained by permuting the elements of  $\tilde{\mathbf{w}}$ . We define a permutation matrix  $\mathbf{P} \in \mathbb{C}^{N_s M^2 \times N_s M^2}$  such that

$$\mathbf{w} = \mathbf{P}\tilde{\mathbf{w}} \quad \text{and} \quad \tilde{\mathbf{y}} = \mathbf{P}^T\mathbf{y} \quad (11)$$

where  $\mathbf{P}$  is a unitary matrix [9]. The permutation matrix  $\mathbf{P}$  converts  $\tilde{\mathbf{w}}$  in the sub-UCA space into  $\mathbf{w}$  in the subarray space at the transmitter, and at the receiver  $\mathbf{P}^T$  brings the received signal  $\mathbf{y}$  in the subarray space back to  $\tilde{\mathbf{y}}$  in the sub-UCA space. This permutation matrix also relates the precoders  $\mathbf{F}$  and  $\tilde{\mathbf{F}}$ , as shown below.

**Lemma 2.** *The precoders  $\mathbf{F}$  in (6) and  $\tilde{\mathbf{F}}$  in (7) are related as*

$$\mathbf{F} = \mathbf{P}\tilde{\mathbf{F}} \quad (12)$$

*Proof.* Since  $\tilde{\mathbf{w}} = \tilde{\mathbf{F}}\mathbf{x}$ , the 1<sup>st</sup> equation in (11) is rewritten as  $\mathbf{w} = \mathbf{P}\tilde{\mathbf{F}}\mathbf{x} = \mathbf{F}\mathbf{x}$ , where the 2<sup>nd</sup> equality comes from (1). This proves (12).  $\square$

Now we are ready to prove **Theorem 1**.

*Proof of Theorem 1.* We first show the identity between  $\mathbf{F}^T\mathbf{y}$  and  $\tilde{\mathbf{F}}^T\tilde{\mathbf{y}}$ . From (11) and (12),  $\mathbf{F}^T\mathbf{y} = (\mathbf{P}\tilde{\mathbf{F}})^T\mathbf{y} = \tilde{\mathbf{F}}^T\mathbf{P}^T\mathbf{y} = \tilde{\mathbf{F}}^T\tilde{\mathbf{y}}$ . This indicates that

$$\tilde{\mathbf{H}} = \mathbf{P}^T\mathbf{H}\mathbf{P} \quad (13)$$

The effective channel in (2) is written as:  $\mathbf{G}^H\mathbf{H}\mathbf{F} = \mathbf{F}^T\mathbf{H}\mathbf{F} = \tilde{\mathbf{F}}^T\mathbf{P}^T\mathbf{H}\mathbf{P}\tilde{\mathbf{F}} = \tilde{\mathbf{F}}^T\tilde{\mathbf{H}}\tilde{\mathbf{F}} = \sum_n \sum_m \tilde{\mathbf{H}}_{nm}$ , where the last equality holds true, because  $\tilde{\mathbf{F}}$  in (7) consists of identity matrices  $\mathbf{I}_{N_s}$ . Thus the effective channel is given by the sum of all circulant matrices in (5), indicating that the effective channel is circulant, because sum of circulant matrices is circulant.  $\square$

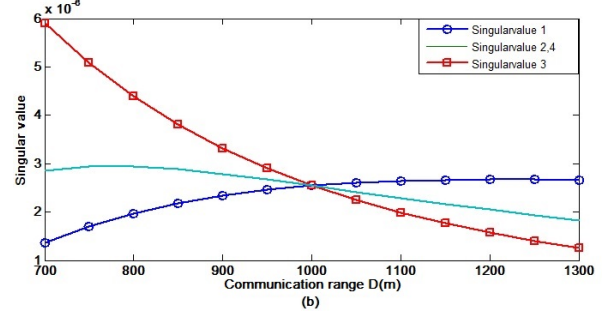
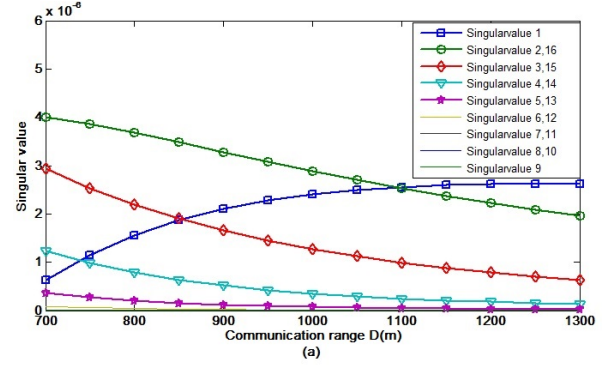


Fig. 5: Singular values. (a) The  $16 \times 16$  UCA. (b) The UCA-SA.

## V. SIMULATION RESULTS

The proposed UCA-SA with constant beamformers is examined through computer simulation. The simulation parameters are as follows:  $N_s = 4$ ,  $M = 2$ , and the carrier frequency is 75GHz ( $\lambda = 2\text{mm}$ ). The communication range is in between 700 and 1300 meters ( $700 \leq D \leq 1300$ ), and the signal-to-noise ratio (SNR) at the receiver is 10dB. The radii of transmit/receive UCAs are determined to satisfy the full rank condition [2]:

$$R_t R_r = \frac{\lambda D}{2N_s \sin^2(\alpha/2)} \quad (14)$$

where  $\alpha = 2\pi/N_s$ . When determining the radii to meet (14), we assume  $R_t = R_r$  and  $D = 1000$  meters. Then for the above simulation parameters, the radii become 1 meter. The proposed UCA-SA is compared with the conventional UCA of the same size (1 meter radii) and the same number of antennas (16 antennas). We employ  $4 \times 4$  and  $16 \times 16$  DFT/IDFT processors for diagonalizing the channels of UCA-SA and the conventional UCA, respectively.

Fig. 5 shows the singular values of the UCA-SA and the  $16 \times 16$  UCA against  $D$ . All the singular values are greater than zero, and thus after diagonalization the UCA-SA and the  $16 \times 16$  UCA have 4 and 16 independent parallel channels, respectively. However, in the case of the  $16 \times 16$  UCA, 7 out of 16 singular values are considerably less than the others and close to zero for all  $D$  values. Consequently, if we perform water-filling power allocation at the transmitter, the number of independent parallel channels which are assigned non-zero

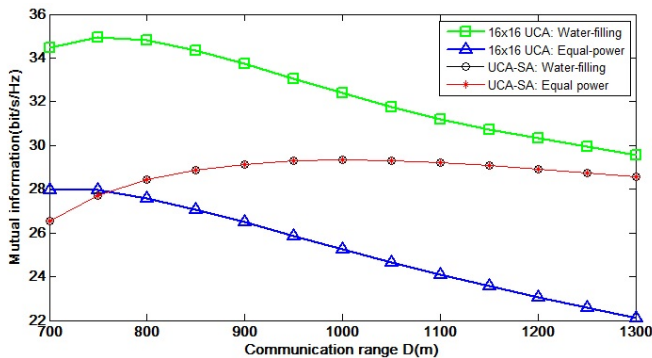


Fig. 6: Mutual information curves for the UCA-SA and the  $16 \times 16$  UCA.

transmit power is less than 9. (In fact, this number reduces to 7 and 5 when  $D \geq 750$  and  $D \geq 1200$ , respectively.) On the other hand, all four singular values of the UCA-SA look significant, and they lead to four independent parallel channels after water-filling power allocation. The four singular values become identical to each other when  $D = 1000$ , due to the full rank condition (14).

Fig. 6 shows the mutual information of the UCA-SA and the  $16 \times 16$  UCA against  $D$ . We consider both equal power allocation and optimal water-filling, where only the former is practical, because the CSI is not available (or equivalently  $D$  is unknown) at the transmitter (the latter is considered for comparison). The water-filling provides the  $16 \times 16$  UCA with 7 bits/sec/Hz gain; however, in the case of the UCA-SA, the gain achieved by water-filling is minor and the two mutual information curves from the two power allocation schemes look overlapped. Comparing the mutual information curves associated with equal power allocation, the UCA-SA outperforms the  $16 \times 16$  UCA when  $D \geq 750$ . In this communication range, the UCA-SA's mutual information curve lies in between those of the  $16 \times 16$  UCA with equal/water-filling power allocations. One notable fact is that the UCA-SA's mutual information remains almost the same for  $D \geq 900$ , while those of the  $16 \times 16$  UCA monotonically decrease with  $D$ . As a result, the mutual information curves of the UCA-SA and the  $16 \times 16$  UCA with water-filling get closer as  $D$  increases. As mentioned above, the  $16 \times 16$  UCA with water-filling exploits only 5 independent parallel channels when  $D \geq 1200$ , and its mutual information is close to that of UCA-SA exploiting 4 independent parallel channels. These results indicate that the UCA-SA is a useful alternative to conventional the  $16 \times 16$  UCA when the CSI is not available at the transmitter.

## VI. CONCLUSION

We proposed the use of UCA-SA for MMW LoS communication and designed optimal beamformers for subarrays. It has been shown that the constant beamformers can make the effective channel of UCA-SA system circulant. The proposed UCA-SA system employs the constant beamformers and diagonalizes the effective channel by DFT/IDFT processors

without the knowledge on CSI at the transmitter. Simulation results demonstrate that the proposed UCA-SA with 4 subarrays consisting of 4 antennas per subarray can outperform the conventional  $16 \times 16$  UCA of the same aperture size.

## REFERENCES

- [1] Peng Wang, Yonghui Li and Vucetic, "Millimeter wave communications with symmetric uniform circular antenna arrays," *IEEE Commun. Lett.*, vol. 18, no. 8, pp. 1307-1310, Aug. 2014.
- [2] Liang Zhou and Yoji Ohashi, "Low complexity millimeter-wave LOS-MIMO precoding systems for uniform circular arrays," in *Proc. IEEE Wireless Communications and Networking Conference (WCNC), Track 1 (PHY and Fundamentals)*, pp. 1293-1297, Istanbul, Turkey, Apr. 2014.
- [3] O. Edfors and A. J. Johansson, "Is orbital angular momentum (OAM) based radio communication an unexploited area?," *IEEE Trans. Antennas and Propag.*, vol. 60, no. 2, pp. 1126-1131, Feb. 2012.
- [4] D. Gesbert, H. Bolcskei, D. A. Gore, and A. J. Paulraj, "Outdoor MIMO wireless channels: models and performance prediction," *IEEE Trans. on Commun.*, vol. 50, no. 12, pp. 1926-1934, Dec 2002.
- [5] F. Bohagen, P. Orten, and G. Oien, "Design of optimal high-rank line-of-sight MIMO channels," *IEEE Trans. Wireless Commun.*, vol. 6, no. 4, pp. 1420-1425, Apr. 2007.
- [6] I. Sarris and A. Nix, "Design and performance assessment of high-capacity MIMO architectures in the presence of a line-of-sight component," *IEEE Trans. Veh. Technol.*, vol. 56, no. 4, pp. 2194-2202, Jul. 2007.
- [7] P. Wang, X. Yuan, Y. Li, L. Song, and B. Vucetic, "Tens of gigabits wireless communications over E-band LoS MIMO channels with uniform linear antenna arrays," *IEEE Trans. Wireless Commun.*, vol. 13, no. 7, pp. 3791-3805, Jul. 2014.
- [8] Eric Torkildson, Upamanyu Madhow, and Mark Rodwell, "Indoor millimeter wave MIMO: feasibility and performance," *IEEE Trans. Wireless Commun.*, vol. 10, no. 12, pp. 4150-4160, Dec. 2011.
- [9] P. P. Vaidyanathan, See-May Phoong, and Yuan-Pei Lin, *Signal Processing and Optimization for Transceiver Systems*. Cambridge University Press, 2010.